Engineering zirconia coating microstructures by using saccharides in aqueous suspension plasma spraying feedstocks

V. Carnicer[a*], M.J. Orts[a], R. Moreno[b], E. Sánchez[a]

[a] Instituto de Tecnología Cerámica (ITC), Universitat Jaume I, 12006, Castellón, Spain

[b] Instituto de Cerámica y Vidrio (ICV), Consejo Superior de Investigaciones Científicas (CSIC), Universidad Autónoma de Madrid, 28049, Madrid, Spain

*Corresponding author at Instituto de Tecnología Cerámica, Campus Universitario Riu Sec. Av. Vicent Sos Baynat s/n, 12006 Castellón, Spain, tel: +34 964 34 24 24. E-mail address: victor.carnicer@itc.uji.es (V. Carnicer)

Abstract

This study aims to demonstrate the feasibility to develop columnar microstructures in YSZ coatings manufactured by suspension plasma spray, through the modification of the properties of the suspension feedstocks with different common monosaccharides: fructose, ribose and glucosamine. The research also pretends to relate the properties of the suspensions to the final coatings. For the study, the saccharides suspensions were characterised in terms of physical and rheological properties. Then, highly concentrated suspensions containing the saccharides were plasma sprayed under the same spraying conditions. The experimental study with optic and scanning electron microscopy was used to evaluate the microstructure of the coatings and their characteristics, while the confocal laser scanning microscope (CLSM) was used to carry out a precise study of the surface topography.

Results showed that saccharides produce a strong influence on the proliferation of columnar structures in the coating cross-section visible as cluster (cauliflower-like) structures on the surface. This effect is due to the diminution of water surface tension as well as an extra energy input during combustion of the saccharides. CLSM has allowed a detailed examination of the topography of the coatings to clearly quantify the differences observed in relation to the development of columnar microstructure.

Keywords: Thermal barrier coatings; saccharides; columnar microstructure; suspension feedstock properties; suspension plasma spray

1. Introduction

In recent years, the optimisation of process engineering has had a remarkable effect on the manufacture of high-performance ceramic coatings and increased operating times due to the study and better understanding of processes, processing variables, surfaces and microstructures of the coatings [1]. The surface of any coating is the first area of contact against the adversities of the environment to which it will be exposed, while the microstructure is of vital importance to obtain properties in accordance with the requirements and to maintain the integrity of the whole system.

By definition [2], thermal barrier coatings (TBC) are layered systems usually comprising two or three layers, used to protect the substrate from high temperatures and extreme operating conditions, and therefore to mitigate degradation and to increase process/work efficiency, such as in engines or turbines. During the last decades, zirconia-based ceramics have been the preferred material in the manufacture of thermal barrier coatings, due to their good thermal properties, although there are currently studies to find alternative materials with similar behaviour [3,4].

Suspension Plasma Spraying (SPS) has become for the last few years one of the most widely addressed techniques in the literature to obtain thermal barrier coatings. The SPS technique is a variant of powder deposition or atmospheric plasma (powder) spraying (APS), where a suspension of particles is injected directly into the plasma torch, allowing the possibility of spraying very fine and non-agglomerated powders [5]. In comparison with other techniques, SPS is a promising, versatile, robust and economical technique, which allows obtaining a variety of tailor-made microstructures from laminar (relatively dense or porous) to columnar (also called cauliflower-like) microstructures, the latter being particularly attractive for TBCs [6–8]. Nowadays, the columnar type microstructure seems to be the most desired microstructure for its use in the protection of internal metal

components of turbines that are in direct contact with high temperature gases. According to many works, this type of microstructure seems to allow longer operation time and resistance to thermal cycles due to the presence of vertical cracks or inter-columnar spaces, which help to decrease the stresses produced by thermal expansion despite the fact that inter-columnar spaces can modify thermal conductivity [9,10]. Therefore, it is essential to understand the formation mechanisms and how to generate columnar-type microstructures together with controlled porosity contents, similar to APS coatings, to achieve a compromise between low conductivity and high resistance to fatigue cycles.

Recently, VanEvery et al. [11] proposed a theory to try to explain the process of columnar formation in the spraying of suspensions, which suggests that columnar development is closely linked to the formation of very fine droplet sizes of suspension on the plasma stream, so that when the solvent (and additives) evaporates very small masses of molten particles are generated. The size decrease of molten particles causes that the gas flow of the torch can modify the direction of the smallest particles during deposition, resulting in different areas of deposition.

Consequently, particles tend to deviate forming preferential deposition zones, related to the surface roughness of the substrate. Although roughness increases the probability of column formation, Sokolowski et al. [12] have developed columnar coatings on smooth polished surfaces. This column creation has been attributed to the fact that the first deposited splats act as initial roughness generators on which the columnar, cauliflower-like microstructure develops.

From the appearance of the SPS technique, a great number of works have focused on the design of microstructural features through the modification of the spraying parameters, architecture of the torch or properties of the substrate, getting promising microstructures with good properties [12–15]. However, the understanding of the effect of the properties

of the suspension feedstock on the microstructure has not been sufficiently treated, particularly in aqueous feedstocks. Thus, Rampon et al. [16] have addressed the effect of rheological properties, while Curry et al. [17] and Ganvir et al. [6] have compared the use of ethanol and water-based suspensions. These works have shown, among other effects, clear benefits for columnar formation in organic-base suspension feedstocks but when the organic solvent is replaced by water the colloidal stability was affected and the formation of the columnar microstructure was minimised or aborted [6,16,17].

Nowadays, there is a great interest in getting higher deposition rates through the use of high solids contents and the employment of aqueous medium, due to environmental and safety considerations, without affecting the columnar formation. This way, in a recent work by the authors, columnar-type microstructures have been successfully obtained in aqueous suspensions by adding fructose as modifier of the rheological properties of the suspension feedstock [18]. According to the state of the art, the addition of some saccharides can be very beneficial because it enhances the dispersion of particles, decreases the surface tension of the solvent and acts as a tailor-made pore-forming agent [19,20]. Additionally, saccharides exhibit the particularity of dissolving easily in polar solvents, being non-toxic and presenting an easy elimination during and after spraying due to the high temperature of the coating process [21].

In previous works [18,22] the use of high solid contents in aqueous suspensions was addressed together with the modification of the spraying distance, while a preliminary, promising study on the addition of a specific saccharide (fructose) was presented and discussed. The purpose of this paper is to study in detail the microstructural effect (morphology, surface roughness and microstructure parameters) produced by the addition of different types of saccharides in a highly concentrated aqueous zirconia suspension. Three common monosaccharides, i.e fructose, ribose and glucosamine were chosen due

to their different chemical structure: hexose, pentose, and amino sugar, respectively. Firstly, the effect of these sugars on the physical and rheological properties of the suspension feedstocks was addressed. Secondly, a completed examination on surface and cross-section of the obtained coatings based on profilometry, confocal laser scanning microscopy and scanning electron microscopy was carried out. Then, correlations between feedstock characteristics and microstructural features of coatings were established.

2. Experimental procedures

2.1 Suspension preparation and characterisation

Suspensions were composed of zirconia doped with 3 mol% Y_2O_3 (TZ-3YS, Tosoh Co., Japan) in deionised water. Average particle diameter of zirconia was about 0.4 μm. Suspensions were dispersed with 0.2 wt% (referred to solids) of an ammonium based polyacrylate (Duramax D3005, Rohm & Haas, USA), according to previous work [23]. Three different types of monosaccharides i.e., D-fructose (AppliChem GmbH, Germany, and labelled F), D-ribose (Merck KGaA, Germany, and labelled R) and glucosamine (VWR International, USA, and labelled G) were used. Each suspension was prepared individually and following the same methodology, in which the solute (saccharide) was initially mixed in the solvent (water) in gentle agitation until it was completely dissolved. Later, the zirconia particles were slowly added in the saccharide-water solution, maintaining the agitation to favour the dispersion of zirconia particles. Subsequently, the suspension was kept in moderate agitation for a few minutes and a stability study was carried out by applying different ultrasound times (UP 400S, Dr Hielscher GmbH, Germany) to guarantee correct dispersion and stability. All saccharides were added in the same concentration in weight (20% respect to solids) to promote a better comparison

among themselves. The solid loading of the suspensions was fixed at 20 vol.% (≈60 wt%) except for glucosamine sugar in which the maximum feasible solid content was decreased down to 10 vol.%.

All solutions and suspensions were characterised to evaluate the effect of saccharides on some properties of water such as surface tension and rheological behaviour. Thus, surface tension was measured by means of a Tensiometer K-12 with a standard plate (KRÜSS GmbH, Germany) and the rheological measurements were carried out with a Haake RS50 rheometer (Thermo, Karlsruhe, Germany) using a double cone-plate geometry and operated in a shear rate mode from 0 s^{-1} to 1000 s^{-1}. More details of these test procedures were described in previous works [18,23]. All samples were tested at controlled room temperature and the experiments were repeated to obtain reliable averages. Finally, zeta potential measurements of dissolved saccharides were determined using Zetasizer Nano-ZS (Malvern, UK). The following nomenclature has been adopted to name the different suspensions during the presentation of the results. The first number 10 or 20 indicates the solids content (in volume), the first letter represents the zirconia ceramic power employed in aqueous suspensions (indicated by Z) and the second letter means the type of saccharides added to prepare the suspensions (F: fructose, R: ribose and G: glucosamine).

2.2 Coatings preparation and characterisation

Before thermal spraying, stainless steel substrates (AISI 304) with the size of 100 mm x 30 mm x 3 mm were cleaned with ethanol to remove dirt and grit blasted using alumina powder (220 grit) at a constant pressure of 4.2 bar. Later, all surface substrates were again cleaned in ethanol and ultrasonic bath to remove possible waste and alumina particles. A NiCoCrAl powder (Amdry 997, Oerlikon Metco, Switzerland) was sprayed as a bond coat on substrates using an F4-MB torch (Oerlikon Metco, Switzerland) coupled with a

six-axis robot (IRB 1400, ABB, Switzerland). The thermal spray conditions to bond coat deposition were supplied by the powder manufacturer. Zirconia topcoats were deposited employing the same torch mentioned above but with an incorporated liquid feeding system to spray suspensions, which was described in previous work [22]. The SPS parameters used during the ceramic topcoat were determined in the previous research with fructose [18] whereas the number of torch scans was increased to ten in order to enlarge the final coating thickness. All samples were sprayed under the same conditions to guarantee suitable comparison, minimise changes in the microstructure due to plasma parameters, and ensure that all changes produced were exclusively due to modifications in the suspension feedstocks.

2.3 Characterisation of coatings roughness and microstructure

All ceramic coatings were characterised to evaluate the effect produced by the suspension feedstock on the surface topography and cross-section microstructure of the coatings.

The analysis of the surface of the coatings was evaluated and compared using confocal laser scanning microscopy, CLSM (LEXT OLS5000, Olympus, Japan) and optical microscopy, OP (BX53M, Olympus, Japan) equipped with a colour camera (DP22, Olympus, Japan) and using an specific free image analysis software (Image J).

First, CLSM was employed to evaluate 3D roughness and volume parameters on coatings using a stripped laser projection with a wavelength of 405 nm and a 20x magnification for data analysis recorder. Secondly, three images of each sample surface were acquired with the OP and digitally treated to calculate the cauliflower-like columnar distribution and the volume of columns (cauliflowers).

In all measurements, three random scan zones with a size of ≈25 mm^2 for each zone were taken from the surface of the coatings in areas sufficiently far from the edges of the

coatings, to avoid errors due to surface direction change. In addition, possible contaminants were removed using ethanol and air pressure before each test.

Finally, specimens were cut from random areas using a diamond cutting blade and metallographically prepared (cleaned, mounted in an epoxy resin and polished) using a Tegramin-25 polishing machine (Struers, Denmark). Later, a cross-section examination was carried out to observe the microstructure, thickness and porosity of the coatings in a field-emission scanning electron microscope (SEM, Quanta 200FEG, FEI Company, USA) along with the mentioned free image analysis software "Image J". Several SEM images at 500x magnification of coatings were statistically analysed using this software. Moreover, a column density measurement (columns/mm) was then calculated according to the procedure described by Ganvir et al. [6], which consists of counting all intersection of the columnar boundaries greater than a half of the coating thickness that crosses a straight line drawn over one half of the coating. A similar procedure has been used to calculate the density of vertical cracks/inter-columnar voids, but in this case, the intersections produced by the vertical cracks/inter-columnar voids were counted [15].

3. Results and discussion

3.1 Physical properties of saccharides solutions

The saccharides were mixed with water to observe the change in surface tension and viscosity of the liquid, as it can be seen in Fig. 1. A significant decrease in surface tension was observed when the amount of any sugar increased until approximately 50%, while for higher contents it increased rapidly. On the contrary, viscosity always grew in the whole tested interval, particularly for concentrations higher than 50%, as expected for the addition of increasing amounts of dissolved chemicals in water, which give rise to a progressive growth of the effective volume of polymer present in the solution. With

regard to surface tension, it decreased with ribose and glucosamine as previously reported for fructose [18]. Although pure sugars are characterised by low surface activity, the common presence of minor components or even impurities is the reason for their surface-active effect when dissolved in water as reported elsewhere [24,25]. Nevertheless, at sufficiently high sugar concentrations, the poor affinity of the sugar to the surface results in a progressive increase in surface tension.

It is important to note that there are no values for glucosamine contents above 30% due to the limited solubility of this sugar. Therefore, the 20% saccharide content in relation to the solids was chosen to prepare all the suspensions to avoid the problem of solubility, whereas low viscosity and surface tension solutions were obtained in all the cases.

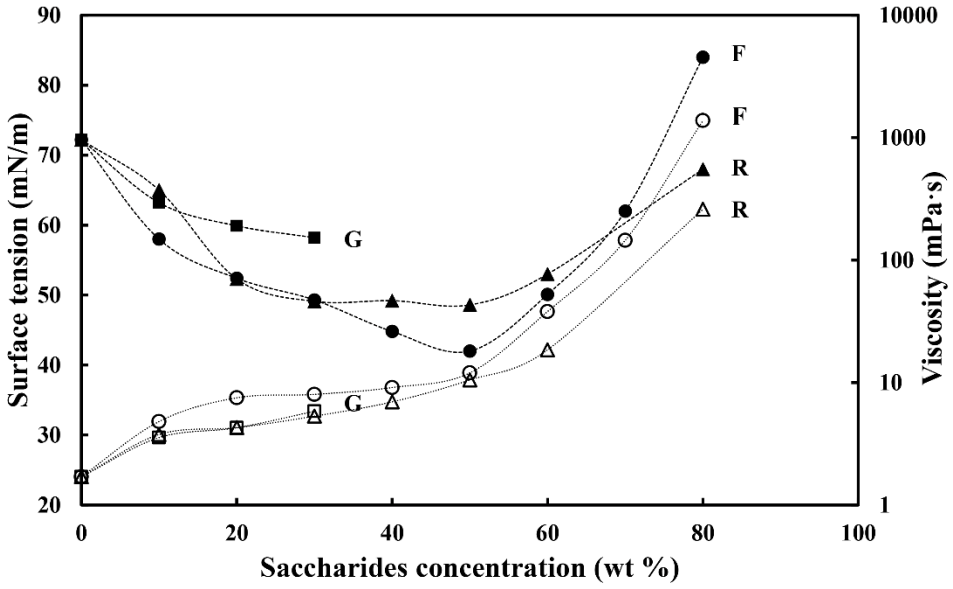

Fig. 1 Evolution of surface tension (full symbol) and viscosity (empty symbol) at 1000s^{-1} with concentration of the different saccharides in water. Circle, triangle and square correspond to fructose, ribose and glucosamine, respectively.

3.2 Colloidal and rheological behaviour of the suspension feedstocks

A colloidal and rheological study of all the zirconia suspensions containing the three sugars was carried in order to assess the stability of the feedstocks. Fig. 2 shows the evolution of zeta potential with pH variation for the suspensions of pure zirconia and

those obtained with the three saccharides added to 20 wt% (with respect to powder). It can be seen that the isoelectric point (referred to as iep) of zirconia with deflocculant occurs at around pH 2.5 while at normal pH of the suspension a good (sufficiently low) zeta potential value (<-55mV at pH ~5.5), is observed as previously reported [23]. The addition of saccharides produces a shift of the zeta potential curve towards higher pH, so that iep is also shifted to the right, from pH 2.5 to 3.6, 3.9 and 4.1 for ribose, fructose, and glucosamine, respectively. This shift of the iep denotes certain interaction of the saccharides with the zirconia particle surface, similarly to that observed with addition of deflocculant or some saccharides [21,22]. Thus, as described by Falkowski et al [21], the effect associated with the addition of monosaccharides to a suspension of ceramic particles (alumina) seems to be due to the displacement of the adsorbed water molecules on the surface, thus it is more a steric effect rather than an electrical one.

Regardless the differences in the iep values associated to the chemical composition of the sugars, the modification of the iep values does not affect the stabilisation of the suspensions at their natural pH (around of 5.7 ± 0.2) because they remain at around -40mV and no sedimentation phenomena were observed, that suggesting that suspensions kept good stability.

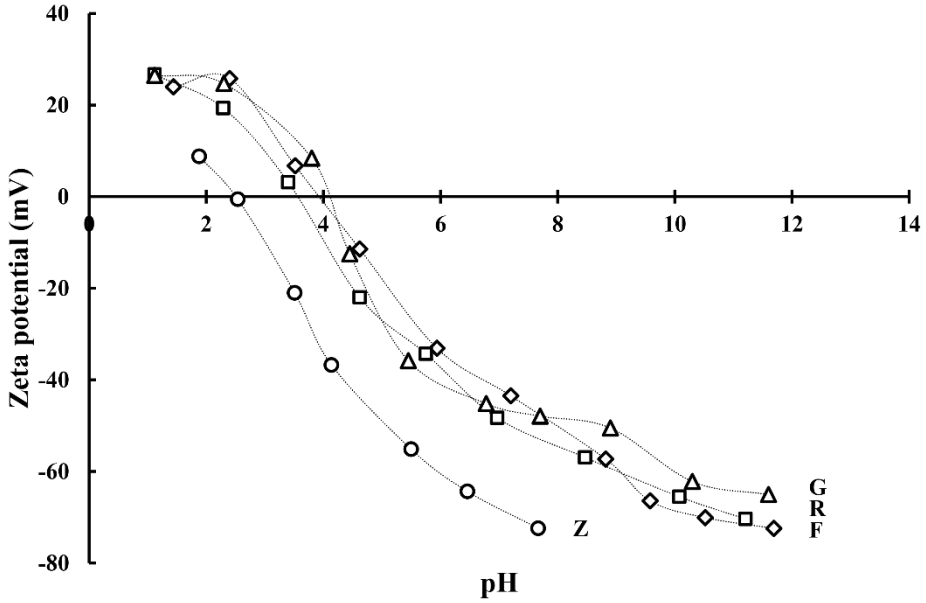

Fig. 2 Evolution of zeta potential of suspensions with the different sugars. Circle, diamond, square and triangle correspond to Y-TZP, fructose, ribose and glucosamine, respectively.

According to the literature [23] and keeping in mind the liquid injection practice, stability control of the suspension feedstock during plasma spraying process is necessary since high viscosity values together with particle agglomeration in the suspension can favour the heterogeneity of the suspension feed during spraying and eventually, the obstruction of the injector nozzle. Therefore, the aim of suspension feedstock preparation must be obtaining a suspension with a viscosity as low as possible and the minimum variation of its rheological properties over time.

Fig. 3 shows the rheological curves for suspensions containing the three sugars and after homogenisation for different sonication times. Solid content of suspensions was 20 vol.% except for G sample where this content had to be decreased down to 10 vol.% due to the difficulty in dispersing the zirconia particles to that solid content because of the high viscosity of the G solution. This reduction of solid content allowed us to maintain similar viscosity ranges for all spraying suspensions so that similar processing conditions can be obtained and therefore, better reliability in the analysis of microstructural features can be

achieved. Besides, a magnification of the curves at high shear rates is also shown to facilitate the display of the graphs. As it can be seen F and R suspensions follow a rheological behaviour which is quite similar to that of zirconia suspension. Thus, for these three suspensions, only mechanical stirring (0 minutes ultrasounds) becomes insufficient to disperse the particles correctly in the liquid medium, giving rise to high viscosities and large thixotropic cycles, which evidence a lack of homogeneity. It is therefore necessary to apply sonication to promote the dispersion of the particles to get homogeneous suspensions. As it is also observed, 1 minute of ultrasounds is enough to get the stabilisation effect by removing the thixotropic area of the curves.

On the other hand, sonicated suspensions show curves with Newtonian behaviour although in the curves of the lowest viscosity samples there is an apparent dilatant behaviour at a high shear rate. This event on flow curves usually occurs in extremely low viscosity fluids (at the limit of the measuring range) by a wall slippage effect between the fluid and the measuring device, as it has been reported elsewhere [26].

With regard to G suspension, its rheological behaviour was different. Despite having to reduce the solids content of the suspension, the application of ultrasound does not result in a completely stable suspension as the thixotropic area is always visible. This exceptional behaviour of glucosamine may be due to the small content of hydrochloric acid as well as the presence of amine group in its chemical composition [27]. The intrinsic flocculation effect of the acid can explain the difficulty in dispersing this sugar.

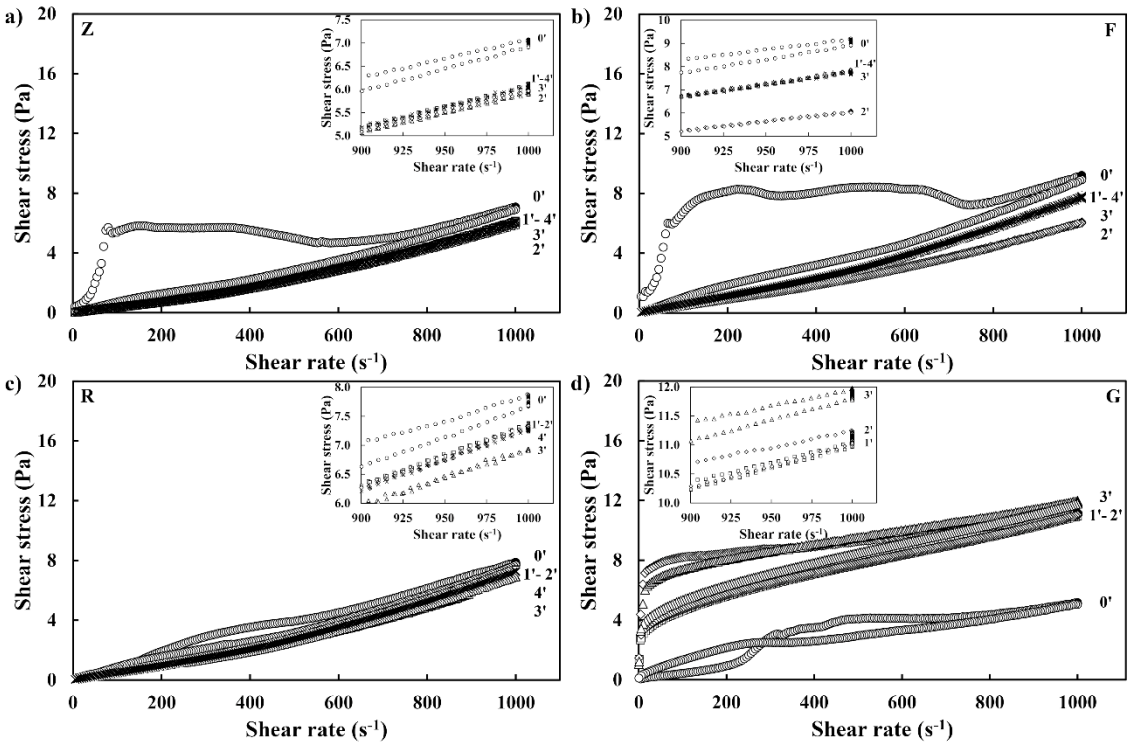

Fig. 3 Comparison of flow curves of YTZP (a) and with saccharides: fructose (b), ribose (c) and glucosamine (g) with different sonication times. The number at right of flow curves represents the minutes of sonication times. Solid loading was 20 vol.% except for G, where it was 10 vol.%.

A summary of viscosity and thixotropy values is presented in Table 1. It can be seen the similarity of data for zirconia and F and R suspensions. Thus, addition of these two sugars to the zirconia suspension hardly affects the rheological behaviour of the original suspension as similar viscosity values were obtained. In addition, the application of 1 minute of ultrasounds produces an important stabilisation effect by strongly decreasing the thixotropy value. In all three cases (Z, F and R) a slight decrease in viscosity can be observed at longer sonication times but without appreciable changes in thixotropy values. For this reason, 1 min sonication time was adapted for the subsequent suspension feedstock preparation. On the other hand, the rheological data observed for G suspensions at either 20 vol% or 10 vol.% confirm the difficulty for dispersing zirconia in this sugar. Finally, a 30-day suspension control was carried out to check the stability of all the

suspensions over time (aging test). The four suspensions with 1 min sonication were chosen, which were kept in slight agitation until the aging monitoring.

It was observed that zirconia, fructose and ribose suspensions hardly age with time since only a small increase in thixotropy was observed but can be considered acceptable for the long ageing period tested. For G suspension the thixotropy increase was higher but viscosity kept in a reasonable low value. Taking into account these results, all the suspensions presented suitable characteristics to be subsequently projected as the typical period from the suspension preparation process to the plasma spraying operation takes normally only 1- or 2-days.

Table 1 Values of viscosity, thixotropy and stability of the suspensions measured at 1000s^{-1}, from curves plotted in Fig. 3.

Suspension / **US time(min)**	**Viscosity (mPa·s) ***					**Thixotropy (Pa/s) ***					**Aging at 30 days**	
	0'	1'	2'	3'	4'	0'	1'	2'	3'	4	Viscosity (mPa·s)	Thixotropy (Pa/s)
20Z	7.1	6.1	5.9	6.0	6.1	2104	14	14	36	11	6.2	87
20ZF	9.2	7.8	6.1	7.9	7.8	3432	22	87	22	33	7.7	75
20ZR	7.9	7.4	7.4	6.9	7.3	463	33	30	-2	29	7.7	7
20ZG	39.4	58.3	--	--	--	12645	6549	--	--	--	--	--
10ZG	5.1	11.0	11.2	12.0	--	--	168	1659	1068	--	11.5	1759

* Optimized suspensions have been underlined

3.3 Microstructure assessment

Fig. 4 shows the micrographs of the surface and section of the coatings obtained under the same spraying conditions. It can be seen that the addition of saccharides to a zirconia suspension has favoured a drastic microstructural change of the coatings from laminar towards a quasi-columnar type microstructure. The appearance of columnar coatings in aqueous suspensions may be based on the decrease in the surface tension of the

suspension, which is produced by the saccharides. According to the literature [6,28], lower surface tension in the suspension favours a much lower droplet momentum, which results in smaller droplet size during atomisation and a higher possibility that the drops change their trajectory due to the influence of the plasma drag which will produce columnar growth. Viscosity is another parameter of suspension feedstock that can influence drop size. However, as observed in Table 1, viscosity of the suspensions with F and R sugars hardly varied in comparison with the original zirconia suspension. In the case of the 10ZG feedstock, an intermediate situation is observed in relation to the formation of the columnar structure probably associated with the lower amount of saccharide in this suspension. Thus, for this feedstock, although the starting viscosity is somewhat higher than that of the other suspensions (see Table 1), there is also a decrease in the surface tension of the solvent that may explain the development of the columnar microstructure. Indeed, the decrease of the liquid surface tension producing finer droplet sizes during fragmentation seems to compensate the enlarging droplet size effect associated to an increase of suspension viscosity.

Another aspect that could have an influence on column formation deals with the combustion enthalpies of organic compounds. It is known that water needs a high energy input to evaporate [26], while organic solvents have lower vaporisation enthalpies as well as they can also act as fuel by contributing combustion energy to the plasma torch. On this basis, the saccharides could contribute a heat input effect during combustion, which would compensate for the high amount of energy used in evaporating the water. Pawlowsky et al [27] suggested that excessive torch temperatures may favour the sublimation of the particles crust, and, therefore, the decrease of particle size during spraying which would result in a greater facility to be dragged by the plasma flows.

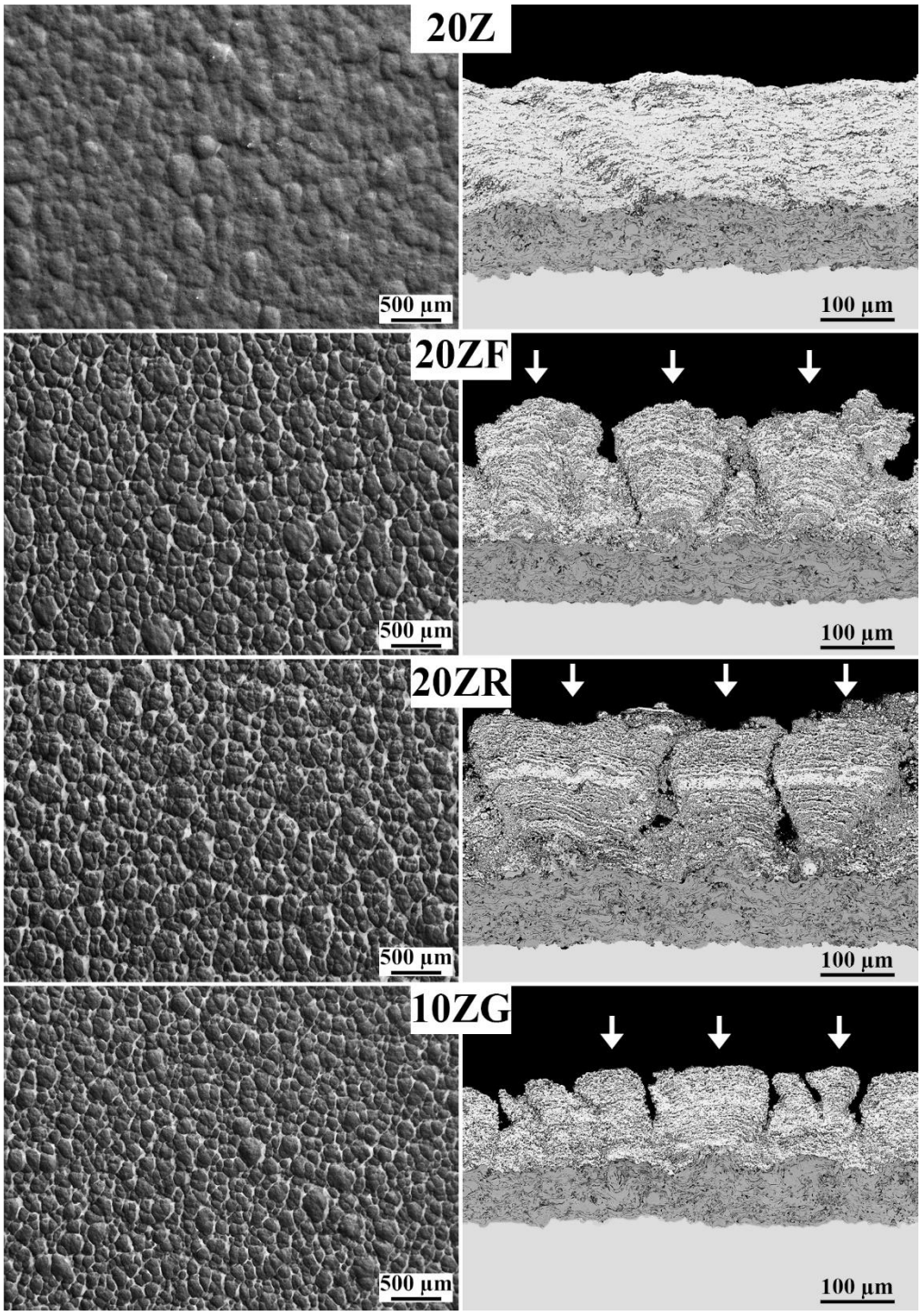

Fig. 4 Surface and cross-section micrographs of the obtained coatings. The white arrows indicate the columns in the coating.

Fig. 5 shows the energy contribution or deficit through the study of the balance of contributions of combustion, vaporisation and melting energies for the different suspension feedstocks, considering their relation solid/liquid/saccharide. The final energy

contribution has been valued as a balance of the energy contributed (input energy) and the energy used (output energy). An input energy value indicates that combustion energy has a greater contribution and compensates for the energy used in the liquid vaporisation and the solid melting. On the contrary, an output energy value means that the vaporisation and melting energy have a greater contribution than that of the combustion energy, and the plasma torch shows an energy loss. For the sake of comparison, the balance assuming ethanol as the only solvent in a hypothetical 20 vol.% YSZ suspension is also included in Fig. 5, and it has been represented as 20ZE. It should be noted that columnar microstructure development is easily achieved when using ethanol as suspension solvent [6,17].

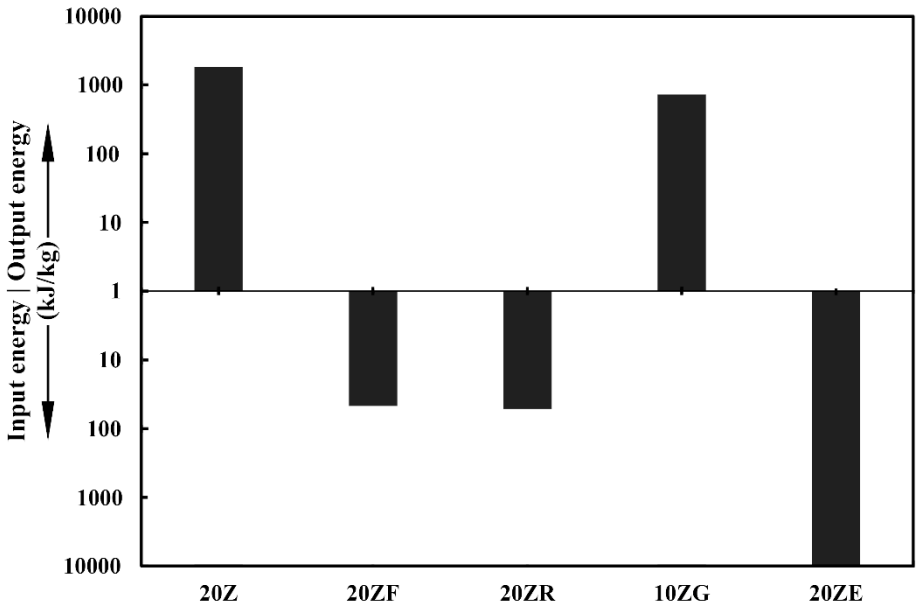

Fig. 5 Comparison of the energy consumed and provided by aqueous suspensions with and without saccharides.

The 20Z suspension has output energy of 1.82 x 10^3 kJ/kg which corresponds to the energy used to evaporate the water (2.6 x 10^3 kJ/kg) and melt the particles (1.3 x 10^3 kJ/kg). While the saccharides have a similar combustion energy around 15.8 x 10^3 kJ/kg,

ethanol has a combustion energy of 29.8 x 10^3 kJ/kg (against 0.9 x 10^3 kJ/kg for its vaporisation energy), i.e. saccharides display an intermediate energy balance between water and ethanol.

As a result, the suspensions with 20 wt% saccharides (20ZF and 20ZR) have an average energy contribution of around 50 kJ/kg, therefore, they compensate the deficit by the evaporation of the water and the melting of the particles, and, besides, they contribute with a small amount of energy to the plasma torch. In the case of the 10ZG feedstock (10 vol.% solids content), the energy contribution was estimated at a half of the previous ones as a result of the similarity in the combustion enthalpies of the three sugars. Somehow, this contribution of energy would have a similar effect to the suspensions to that of organic solvent, although the latter presents much greater values.

In the case of ethanol suspensions, this contribution is estimated at around 10.6 x 10^3 kJ/kg for a suspension with the same characteristics to those of 20Z. Therefore, a possible sublimation effect of the particles due to an extra energy provided by the combustion of organic compounds (saccharides) can also contribute together with the surface tension decrease (droplet generation) to develop the columnar microstructures in these aqueous suspensions.

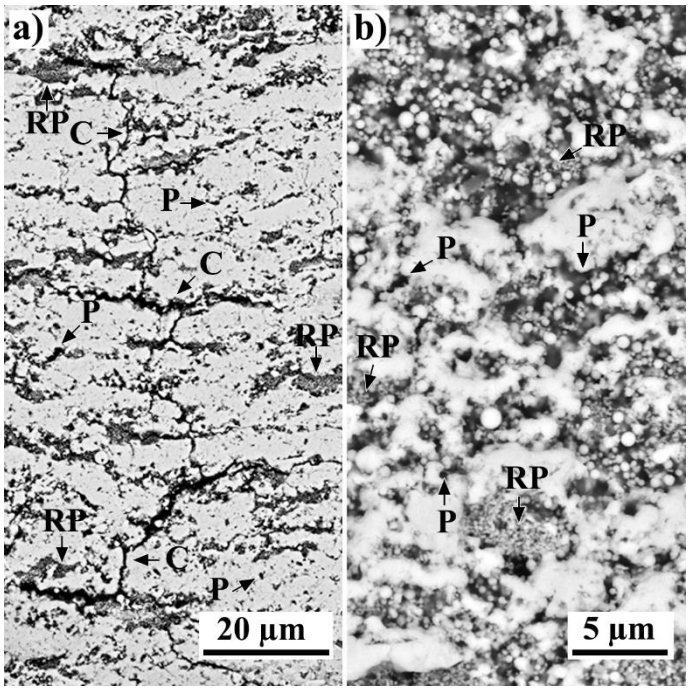

Fig. 6 Example of microstructural details of coatings at different magnifications: a) 20Z and b) 20ZF. Vertical cracks, porosity and resolidified particles are indicated by means of number C, P and RP, respectively.

On the other hand, the coatings show differences between them as it can be seen in Fig. 4 or more precisely in Fig. 6 where some micrographs were magnified. In this Fig. 6 only the 20Z and 20ZF coatings are shown as an example of the internal microstructure of the coatings, the other 20ZR and 10ZG coatings are not shown because they are relatively similar to 20ZF. Related to these figures, Table 2 and Fig. 7, show some microstructural features quantified by means of image analysis. Thus, Table 2 displays some typical characteristics of thermal spray coatings, namely thickness, porosity and the amount of resolidified particles which were insufficiently melted during spraying [22,29] whereas Fig. 7 shows some microstructure features associated with columnar development as reported elsewhere [15].

The 20Z coating showed a laminar type structure with a thickness of around 167 µm and the appearance of different vertical and horizontal cracks sporadically (marked C in Fig.

6), which are only noticeable at higher magnification as previously reported [30]. Crack generation in the coatings may be due to the release of stresses produced during splat deposition [30]. The amount of porosity (marked P in the micrograph) and resolidified particles (marked RP) of this coating were the lowest of all the coatings tested, whereas these were found in the inter-pass areas forming small accumulations (see Fig. 6). Discussions on the identification and quantification of these microstructural features,i.e, porosity and resolidified particles have been extensively reported in the literature on SPS coatings [15,29]. In addition, and as expected due to the characteristics of an aqueous suspension, no columns were observed in the cross-section of the coating and only some clusters were visible on the surface of the coating, owing to the roughness of the coating itself.

Table 2 Microstructural characteristics of coatings with and without saccharides.

Coating	Thickness (µm)	Porosity (%)	Resolidified particles (%)
20Z	167 ± 6	8 ± 31	12 ± 1
20ZF	168 ± 8	14 ± 4	25 ± 3
20ZR	190 ± 8	19 ± 3	39 ± 4
10ZG	126 ± 4	19 ± 3	18 ± 2

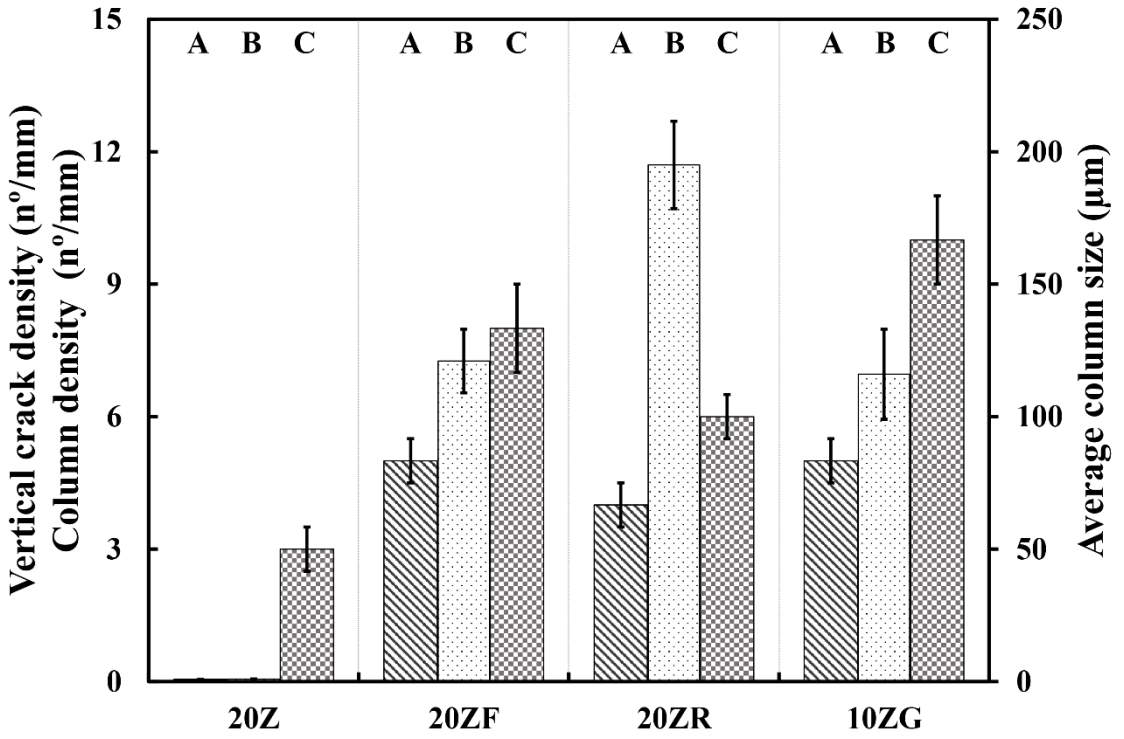

Fig. 7 Comparison of microstructural characteristics in the section of coatings. The display shows the column density (A), the average column size (B) and the density of vertical cracks or inter-column voids (C) represented by striped columns, light columns with dark dots and a pattern of squares, respectively.

In the 20ZF coating, well-defined columns and porous structure can be observed, as previously reported in the literature for this type of coating [18] exhibiting a column size of 121 ± 24 µm and an average column density of 5 ± 1 columns/mm (see Fig. 7). It can be noted that this coating has small gaps in the inter-column voids or vertical cracks, as structures in the form of an inverted cone can be observed, which are only visible in this condition. The thickness of the coating is practically the same as in the 20Z coating but with higher porosity and more resolidified particles (see Table 2). A comparison of the 20ZR coating with the 20ZF coating shows the following: slightly higher porosity, higher thickness probably associated with a more efficient coating deposition, an increase of resolidified particles and a slightly lower presence of cracks or intercolumn spaces as also observed in Fig. 4 and Fig. 6. The 20ZR coating presented the maximum column

thickness (195 ± 33 μm) and the minimum columns density (4 ± 1 column/mm). The lower number of columns could be a consequence of the great thickness of the columns, which would make the appearance of new columns more difficult.

Overall, 20ZF and 20ZR coatings display well developed columnar microstructure characterised by higher porosity and higher amount of resolidified particles in comparison with 20Z suspension as a consequence of the amount of sugar added. On one hand, sugars act as pore formers during spraying leading to porosity increase. On the other hand, the addition of a significant amount of sugar enhances particle resolidification, which would indicate a lower penetration of the liquid into the plasma jet and a larger proportion and distribution of droplet sizes (cloud of vaporisation) at the periphery of the jet, which will be rapidly dragged and cooled by the outermost plasma flow as reported elsewhere [16]. Vertical crack density associated with columnar structure also grows. Finally, although 10ZG coating displays similar porosity as that of 20ZF and 20ZR samples, it is thinner and contains much lower amount of resolidified particles. These characteristics are probably related to the lower solids content, compared to the concentrated suspensions of the 20ZF and 20ZR coatings. As observed in previous works, as the solid concentration of a given suspension feedstock decreases the resulting coating becomes more porous and thinner and contains less resolidified particles as a consequence of the lower amount of suspended particles fed into the plasma torch [12,17,22]. It can also be noted that this coating exhibits a very heterogeneous column thickness (116 ± 34 μm), as observed in the micrograph, while the column density (5 ± 1 columns/mm) is similar to that of the other coatings.

Although small differences are observed in the microstructural characteristics of the coatings obtained from the 20ZF and 20ZR suspensions, in general it can be concluded that these feedstocks lead to coatings in which the columnar structure is clearly

developed, as a consequence of the similarity in the initial characteristics of the starting suspensions and their energetic contribution to the plasma. The small differences observed may, to some extent, be related to the variations observed during the thermal projection experiments as well as to the intrinsic characteristics of the feedstocks. On the other hand, the lower solid concentration and amount of added sugar of 10ZG suspension resulted in a sort of intermediate situation between 20Z and 20ZF and 20ZR coatings in terms of columnar microstructure development.

Surface observation of 20ZF and 20ZR coatings confirms the abundant presence of clusters (cauliflower-like surface) and sub-clusters (or secondary cauliflowers) which are certainly associated with the corresponding columns as extensively reported in the literature [10]. It can also be noticed that the fructose coating shows a greater presence of subclusters and a greater heterogeneity between clusters and subclusters as it could be expected from the cross-section observation. These surface differences or roughness will be dealt with in detail later on. For 10ZG coating the surface view confirms that the coating presents a cauliflower morphology halfway between the initial coating and the other saccharides, but with a more heterogeneous cauliflower size distribution.

It is important to note that the appearance of columns indicates that saccharides have an effect on the formation of finer droplets which exhibit a much smaller droplet momentum. Moreover, an increase in resolidified particles in connection with the appearance of columns was also observed. This related effect would confirm the hypothesis that smaller droplets are being generated and that they are more influenced by plasma flow as observed by Ganvir et al in ethanol suspensions [6].

3.4 Topographical analysis of columnar microstructure development

The confocal laser scanning microscope was used to obtain two (2D) and three-dimensional images (3D) and measure accurately the surface and roughness parameters produced by the addition of saccharides. Topography images obtained have been treated under the same scale to facilitate their comparison, and in which a value of +45 μm has been fixed for the zones of greater height (cauliflower) and value of -55 μm for the zones of greater depth (valleys). In Fig. 8 it can be seen that the coating 20Z presents a low amount of clusters/cauliflowers on the surface, which correspond to 13% of the area. In addition, these clusters are isolated without a continuity towards the interior of the coating, as it can be seen in the cross-section of Fig. 4, therefore they do not contribute to columns development. The addition of fructose and ribose causes a strong surface modification giving rise to the proliferation of a greater number of coarser cauliflowers. In these coatings, the area covered by cauliflowers strongly increases over 65% in both coatings (see Table 3). It is interesting to note that both coatings show a greater variation in the height between the surface of the cauliflowers and the depth of the valley (as shown by the more intense peak colours), indicating the appearance of more defined and deeper inter-columnar voids. The addition of glucosamine leads to a minor topographical modification than that of the other saccharides with a cauliflower-like structure area of 45% (see Table 3). However, in this coating the proliferation of a large number of cauliflowers but of smaller size can be observed in Fig. 8.

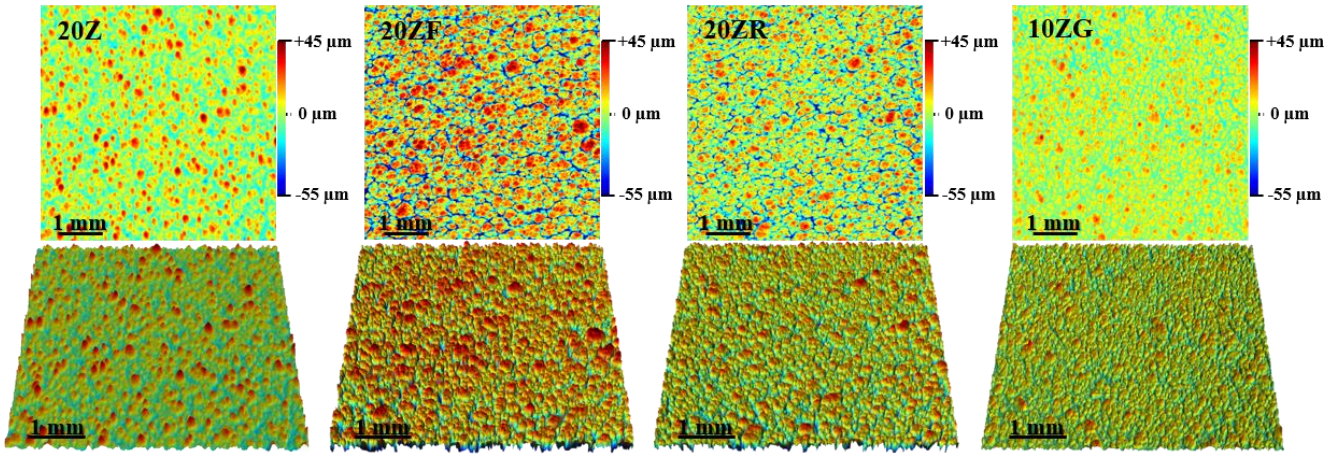

Fig. 8 2D (top) and 3D (bottom) topographies of the different coatings obtained by CSLM.

Fig. 9 shows the size distribution of the cauliflowers on the surface calculated from Fig. 8 topographies. As it can be seen, the original coating (20Z) displays significant clusters of very small size and, as shown in Fig. 8, some isolated roughness of a larger size, which, as mentioned above, correspond to the surface roughness of the coating itself. Fig. 9 also confirm the significant proliferation of cauliflowers that had been previously observed in the 20ZF and 20ZR samples. In addition, although these two coatings present similar cauliflower size distribution there also exists some differences in the 100-200 µm range where 20ZR coating display coarser cauliflowers, confirming observations in Fig. 4 and Fig. 8. Finally, 10ZG curve has an intermediate trend compared to the other curves (20Z and 20ZF) but with a lower number of large cauliflowers. Besides, it should be taken into account that the area covered by cauliflowers in 10ZG coating was much lower than that of 20ZF and 20ZR samples (see Table 3).

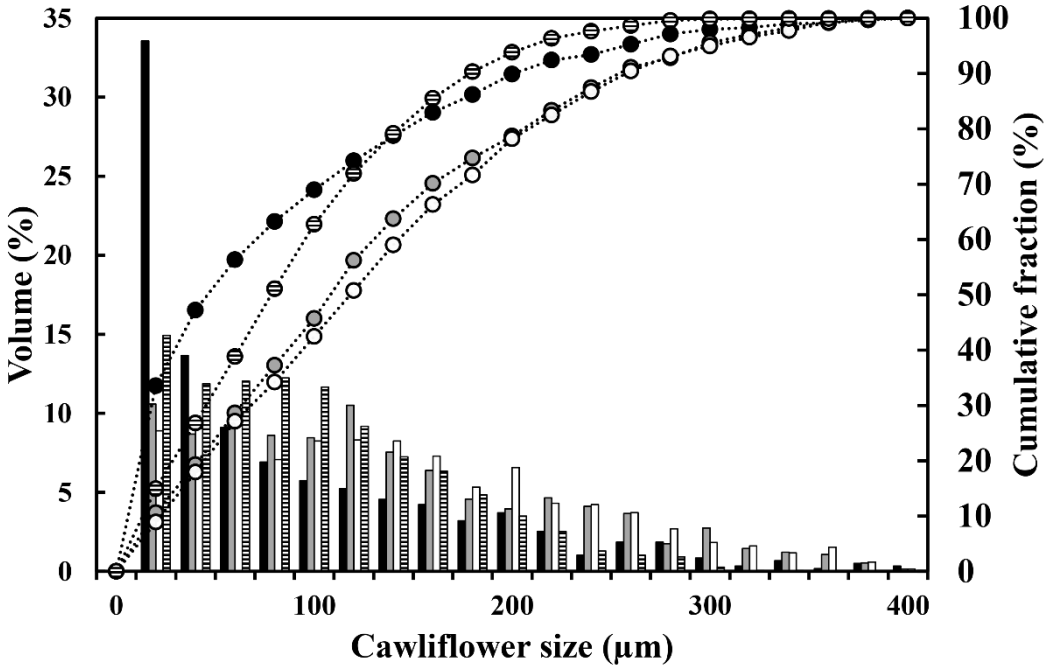

Fig. 9 Size distribution of cauliflower-like structures for the different coatings.The colours black, grey and white and striped lines correspond to the coatings 20Z, 20ZF, 20ZR and 10ZG, respectively.

Table 3 shows a comparison of different roughness values, such as Sa (arithmetic average height of the area) and Sq (root mean square height of the area) obtained from CSLM for the four coatings. As observed, it is quite clear again that the addition of saccharides exerts a direct influence on the roughness. Thus, the sample 20Z displays lower roughness as revealed by Sa and Sq values, while fructose and ribose coatings practically double the value of the sample 20Z, corroborating the development of cauliflower texture as seen in the previous topography and surface images. Roughness values for 10ZG coating also confirm the previous findings when compared with those of the original 20Z as well as 20ZF and 20ZR samples.

Table 3 Coating roughness parameters obtained with CLSM. Sa: arithmetic mean height, Sq: mean square root height and Sz: maximum surface height.

Coating	Sa (µm)	Sq (µm)	Sz (µm)	Surface occupied by cluster structure (%)
20Z	8.0 ± 0.3	10.3 ± 0.2	63.9 ± 4	13 ± 1
20ZF	16.3 ± 2	21.2 ± 2	164.6 ± 10	65 ± 2
20ZR	14.2 ± 1	18.1 ± 2	135.1 ± 4	65 ± 1
10ZG	12.9 ± 3	15.5 ± 3	68.7 ± 9	45 ± 2

Table 3 also shows the changes in the maximum surface height (Sz) which includes the maximum peak and valley height. It is worth noting the similarity of the Sz values between the 20Z and 10ZG sample, which indicates that the coatings have a similar maximum height, although the 10ZG sample was partially (45% of surface) covered by cauliflowers, which resulted in higher roughness (Sa and Sq values). Fructose and ribose coatings double the Sz value of the non-saccharide sample, which is consistent with the greater amount and size of cauliflowers on the surface (greater colour difference in Fig. 8) of these samples. The higher value of 20ZF sample could be attributed to a greater height difference between cauliflower peaks and deep valleys, emphasised by slightly more spaced and deeper inter-column gaps, as observed in Fig. 4 and Fig. 8.

4. Conclusions

This study aimed to obtain columnar microstructures from water based YSZ suspensions by adding saccharides, as modifying agents of the suspension feedstock properties at fixed plasma spray parameters. The changes in the coatings showed:

- The feasibility of using three common monosaccharides, fructose, ribose and glucosamine which produced significant changes in the surface tension of the suspensions

but only slight increase in viscosity (except glucosamine), without practically affecting the stability of the suspension with time. High (20 vol.%) solid content YSZ suspensions containing 20 wt% of sugar were obtained for fructose and ribose but only 10 vol.% solids was possible for glucosamine

- The addition of saccharides managed to develop columnar microstructure from typical laminar-like microstructure with vertical cracks of the SPS YSZ coating obtained from an aqueous suspension. The effect was particularly evident when using fructose and ribose due to the higher sugar content in the feedstocks.
- An exhaustive analysis of columnar development has been carried out by confocal laser scanning microscopy, CLSM. This technique has allowed a detailed examination of the topography of the samples by quantifying the size and distribution of the cauliflowers, as the columns are called from the surface. The topographical observation has made it possible to conclude that in the case of the coatings obtained from fructose and ribose suspensions, 65% of the surface was covered by cauliflowers with an average size ranging from 100 to 200 μm. The results are consistent with those observed by scanning electron microscopy. The parameters of the surface topography allow to clearly quantify the differences observed between the roughness of the samples in relation to the development of the columnar microstructure

The results show the viability of the use of saccharides to obtain columnar microstructures in aqueous suspensions, on the basis of a decrease in liquid surface tension in the feedstock that would favour greater spraying of finer sizes droplets, and the extra energy contribution produced by the combustion of the saccharides.

5. Acknowledgments

All the authors would like to thank the support received by the Spanish Ministry of Science, Innovation and Universities and FEDER Funds, through the research project (ref. RTI2018-099033-B-C31 and C33). V. Carnicer would like to acknowledge to the Research Promotion Plan of the University Jaume I for the predoctoral fellowship (ref. PREDOC/2017/51). Moreover, all authors would also like to thank Paulina Bednarek for her helpful discussions and approach to the saccharides.

References

[1] R. Moreno, Better ceramics through colloid chemistry, J. Eur. Ceram. Soc. 40 (2019) 559–587. doi:10.1016/j.jeurceramsoc.2019.10.014.

[2] D.R. Clarke, M. Oechsner, N.P. Padture, Thermal-barrier coatings for more efficient gas-turbine engines, MRS Bull. 37 (2012) 891–898. doi:10.1557/mrs.2012.232.

[3] R. Vassen, M.O. Jarligo, T. Steinke, D.E. Mack, D. Stöver, Overview on advanced thermal barrier coatings, Surf. Coatings Technol. 205 (2010) 938–942. doi:10.1016/j.surfcoat.2010.08.151.

[4] G. Mauer, M.O. Jarligo, D.E. Mack, R. Vassen, Plasma-sprayed thermal barrier coatings: New materials, processing issues, and Solutions, J. Therm. Spray Technol. 22 (2013) 646–658. doi:10.1007/s11666-013-9889-8.

[5] A. Vardelle, C. Moreau, J. Akedo, H. Ashrafizadeh, C.C. Berndt, J.O. Berghaus, M. Boulos, J. Brogan, A.C. Bourtsalas, A. Dolatabadi, M. Dorfman, T.J. Eden, P. Fauchais, G. Fisher, F. Gaertner, M. Gindrat, R. Henne, M. Hyland, E. Irissou, E.H. Jordan, K.A. Khor, A. Killinger, Y.C. Lau, C.J. Li, L. Li, J. Longtin, N. Markocsan, P.J. Masset, J. Matejicek, G. Mauer, A. McDonald, J. Mostaghimi, S.

Sampath, G. Schiller, K. Shinoda, M.F. Smith, A.A. Syed, N.J. Themelis, F.L. Toma, J.P. Trelles, R. Vassen, P. Vuoristo, The 2016 Thermal Spray Roadmap, J. Therm. Spray Technol. 25 (2016) 1376–1440. doi:10.1007/s11666-016-0473-x.

[6] A. Ganvir, R.F. Calinas, N. Markocsan, N. Curry, S. Joshi, Experimental visualization of microstructure evolution during suspension plasma spraying of thermal barrier coatings, J. Eur. Ceram. Soc. 39 (2019) 470–481. doi:10.1016/j.jeurceramsoc.2018.09.023.

[7] P. Sokołowski, P. Nylen, R. Musalek, L. Łatka, S. Kozerski, D. Dietrich, T. Lampke, L. Pawłowski, The microstructural studies of suspension plasma sprayed zirconia coatings with the use of high-energy plasma torches, Surf. Coatings Technol. 318 (2017) 250–261. doi:10.1016/j.surfcoat.2017.03.025.

[8] R. Musalek, J. Medricky, T. Tesar, J. Kotlan, Z. Pala, F. Lukac, K. Illkova, M. Hlina, T. Chraska, P. Sokolowski, N. Curry, Controlling microstructure of Yttria-stabilized zirconia prepared from suspensions and solutions by plasma spraying with High feed rates, J. Therm. Spray Technol. (2017) submitted. doi:10.1007/s11666-017-0622-x.

[9] B. Bernard, A. Quet, L. Bianchi, A. Joulia, A. Malié, V. Schick, B. Rémy, Thermal insulation properties of YSZ coatings: Suspension Plasma Spraying (SPS) versus Electron Beam Physical Vapor Deposition (EB-PVD) and Atmospheric Plasma Spraying (APS), Surf. Coatings Technol. 318 (2017) 122–128. doi:10.1016/j.surfcoat.2016.06.010.

[10] B. Bernard, L. Bianchi, A. Malié, A. Joulia, B. Rémy, Columnar suspension plasma sprayed coating microstructural control for thermal barrier coating application, J. Eur. Ceram. Soc. 36 (2016) 1081–1089. doi:10.1016/j.jeurceramsoc.2015.11.018.

[11] K. Vanevery, M.J.M. Krane, R.W. Trice, H. Wang, W. Porter, M. Besser, D. Sordelet, J. Ilavsky, J. Almer, Column formation in suspension plasma-sprayed coatings and resultant thermal properties, J. Therm. Spray Technol. 20 (2011) 817–828. doi:10.1007/s11666-011-9632-2.

[12] P. Sokołowski, S. Kozerski, L. Pawłowski, A. Ambroziak, The key process parameters influencing formation of columnar microstructure in suspension plasma sprayed zirconia coatings, Surf. Coatings Technol. 260 (2014) 97–106. doi:10.1016/j.surfcoat.2014.08.078.

[13] O. Aranke, M. Gupta, N. Markocsan, X.H. Li, B. Kjellman, Microstructural Evolution and Sintering of Suspension Plasma-Sprayed Columnar Thermal Barrier Coatings, J. Therm. Spray Technol. 28 (2019) 198–211. doi:10.1007/s11666-018-0778-z.

[14] J. Ekberg, A. Ganvir, U. Klement, S. Creci, L. Nordstierna, The Influence of Heat Treatments on the Porosity of Suspension Plasma-Sprayed Yttria-Stabilized Zirconia Coatings, J. Therm. Spray Technol. 27 (2018) 391–401. doi:10.1007/s11666-017-0682-y.

[15] A. Ganvir, N. Curry, S. Björklund, N. Markocsan, P. Nylén, Characterization of Microstructure and Thermal Properties of YSZ Coatings obtained by Axial Suspension Plasma Spraying (ASPS), J. Therm. Spray Technol. 24 (2015) 1195–1204. doi:10.1007/s11666-015-0263-x.

[16] R. Rampon, O. Marchand, C. Filiatre, G. Bertrand, Influence of suspension characteristics on coatings microstructure obtained by suspension plasma spraying, Surf. Coatings Technol. 202 (2008) 4337–4342. doi:10.1016/j.surfcoat.2008.04.006.

[17] N. Curry, K. VanEvery, T. Snyder, J. Susnjar, S. Bjorklund, Performance Testing

of Suspension Plasma Sprayed Thermal Barrier Coatings Produced with Varied Suspension Parameters, Coatings. 5 (2015) 338–356. doi:10.3390/coatings5030338.

[18] V. Carnicer, F. Martinez-Julian, M.J. Orts, E. Sánchez, R. Moreno, Effect of fructose-containing feedstocks on the microstructure of multicomponent coatings deposited by suspension plasma spraying, J. Eur. Ceram. Soc. 39 (2019) 3433–3441. doi:10.1016/j.jeurceramsoc.2019.04.042.

[19] P. Wiecinska, A. Wieclaw, F. Bilski, Selected sugar acids as highly effective deflocculants for concentrated nanoalumina suspensions, J. Eur. Ceram. Soc. 37 (2017) 4033–4041. doi:10.1016/j.jeurceramsoc.2017.05.037.

[20] M. Montero, T. Molina, M. Szafran, R. Moreno, M.I. Nieto, Alumina porous nanomaterials obtained by colloidal processing using d-fructose as dispersant and porosity promoter, Ceram. Int. 38 (2012) 2779–2784. doi:10.1016/j.ceramint.2011.11.048.

[21] P. Falkowski, P. Bednarek, A. Danelska, T. Mizerski, M. Szafran, Application of monosaccharides derivatives in colloidal processing of aluminum oxide, J. Eur. Ceram. Soc. 30 (2010) 2805–2811. doi:10.1016/j.jeurceramsoc.2010.03.003.

[22] V. Carnicer, M.J. Orts, R. Moreno, E. Sánchez, Influence of solids concentration on the microstructure of suspension plasma sprayed Y-TZP/Al_2O_3/SiC composite coatings, Surf. Coatings Technol. 371 (2019) 143–150. doi:10.1016/j.surfcoat.2019.01.078.

[23] V. Carnicer, C. Alcazar, E. Sánchez, R. Moreno, Aqueous suspension processing of multicomponent submicronic Y-TZP/Al_2O_3/SiC particles for suspension plasma spraying, J. Eur. Ceram. Soc. 38 (2018) 2430–2439. doi:10.1016/j.jeurceramsoc.2018.01.006.

[24] J.W. Russo, M.M. Hoffmann, Influence of typical impurities on the surface tension measurements of binary mixtures of water and the ionic liquids 1-butyl-3-methylimidazolium tetrafluoroborate and chloride, J. Chem. Eng. Data. 55 (2010) 5900–5905. doi:10.1021/je100949x.

[25] M.C. Amiri, A.A. Dadkhah, On reduction in the surface tension of water due to magnetic treatment, Colloids Surfaces A Physicochem. Eng. Asp. 278 (2006) 252–255. doi:10.1016/j.colsurfa.2005.12.046.

[26] R. Moreno Botella, Reología de suspensiones cerámicas, Consejo Superior de Investigaciones Científicas, Madrid, 2005.

[27] P. Falkowski, M. Szafran, Role of molecular structure of monosaccharides on the viscosity of aqueous nanometric alumina suspensions, Ceram. Int. 42 (2016) 8572–8580. doi:10.1016/j.ceramint.2016.02.085.

[28] B. Bernard, A. Quet, L. Bianchi, V. Schick, A. Joulia, A. Malié, B. Rémy, Effect of Suspension Plasma-Sprayed YSZ Columnar Microstructure and Bond Coat Surface Preparation on Thermal Barrier Coating Properties, J. Therm. Spray Technol. 26 (2017) 1025–1037. doi:10.1007/s11666-017-0584-z.

[29] V. Carnicer, M.J. Orts, R. Moreno, E. Sánchez, Microstructure assessment of suspension plasma spraying coatings from multicomponent submicronic Y-TZP/Al_2O_3/SiC particles, Ceram. Int. 44 (2018) 12014–12020. doi:10.1016/j.ceramint.2018.03.186.

[30] R. Vassen, H. Kaner, G. Mauer, D. Stöver, Suspension plasma spraying: Process characteristics and applications, J. Therm. Spray Technol. 19 (2010) 219–225. doi:10.1007/s11666-009-9451-x.